Talanta 100 (2012) 113–122

Contents lists available at SciVerse ScienceDirect

Talanta

journal homepage: www.elsevier.com/locate/talanta

Impurity profiling of capreomycin using dual liquid chromatography coupled to mass spectrometry

Shruti Chopra, Murali Pendela, Jos Hoogmartens, Ann Van Schepdael, Erwin Adams *

Laboratory for Pharmaceutical Analysis, Faculteit Farmaceutische Wetenschappen, Katholieke Universiteit Leuven, Herestraat 49, B-3000 Leuven, Belgium

ARTICLE INFO

Article history:
Received 11 April 2012
Received in revised form
27 July 2012
Accepted 31 July 2012
Available online 7 August 2012

Keywords:
Capreomycin
LC/MS
Impurity characterization

ABSTRACT

The characterization of unknown (UNK) impurities in capreomycin (CMN) using liquid chromatography coupled to mass spectrometry (LC/MS) has been described. The ion-pair liquid chromatography method coupled to ultraviolet detection (LC–UV) described by Mallampati et al. was used for the separation of CMN from its related substances. As the method uses non-volatile reagents it could not be directly coupled to mass spectrometry (MS) for impurity characterization. So, these UNK impurities were collected and desalted before sending to MS for structural characterization. As no information about the fragmentation of the main components of CMN, except for CMN IB, was available in the literature, they were studied first. Next, the structures of the impurities were deduced by comparing their fragmentation to that of the main components of CMN. Fourteen UNK impurities that were never described before, were (partly) characterized.

1. Introduction

Capreomycin (CMN) is an antitubercular antibiotic that belongs to the tuberactinomycin (TUB) family of nonribosomal peptide antibiotics [1]. It is produced by fermentation from *Streptomyces capreolus* and was isolated for the first time by Herr and co-workers in 1959 [2]. CMN was found to have good clinical utility as a second-line antituberculosis drug for treatment of multidrug resistant tuberculosis (MDR-TB) when resistance to first line drugs such as isoniazid, ethambutol and *p*-aminosalicylic acid is developed. Its medical significance is evident by the fact that it is on the World Health Organization's (WHO) list of essential drugs for the treatment of MDR-TB [1].

CMN is a polypeptide composed of nonproteinogenic amino acids that are biosynthesized by a nonribosomal peptide synthetase mechanism [3]. It is characterized by the presence of a cyclic pentapeptide structure and consists of four main active components (IA, IB, IIA and IIB) which are present in approximate percentages of 25%, 67%, 3% and 6% [4]. Structures of the four main components of CMN, its structural analog viomycin (VIO) and the constituent amino acids are shown in Fig. 1. The arabic numbers in the structure of CMN indicate the position of the different AAs that form the pentapeptide ring. These AAs are further described in the text as residue along with their number indicated in the structure. The cyclic pentapeptide ring of all CMNs is composed of two 2,3-diaminopropionic acid (DAP) molecules (residues 1 and 3), the α,β-unsaturated amino acid β-ureido-dehydroalanine (residue 4), an unusual amino acid L-capreomycidine (residue 5) containing a cyclic guanidine moiety (2-amino dihydropyrimidine) and a serine (residue 2) in IA and IIA which is replaced by alanine (residue 2) in IB and IIB. Beside the above described AAs, CMN IA and IB also contain an additional AA, β-lysine (residue 6), which is attached to the β-amino group of residue 3, by a peptide bond which is absent in IIA and IIB [5]. Liquid chromatography (LC) has been used several times for the content determination of CMN. The United States Pharmacopeia and the British Pharmacopoeia recommend microbiological turbidimetric assay and normal phase liquid chromatographic methods for the content determination of CMN [6,7]. Reversed phase (RP) chromatography with ultraviolet detection (UV) has been suggested as an alternative by Rossi et al. for CMN assay in liposomal formulations [8]. For related substances of CMN, a thin layer chromatography method has been described by Lee et al. [9]. Besides chromatography, capillary electrophoresis has been used for the determination of CMN along with ofloxacin

Abbreviations: AA, Amino acid; ACN, Acetonitrile; arb, Arbitrary units; CMN, Capreomycin; CEL, Collision energy level; CID, Collision-induced dissociation; DAP, 2,3-diaminopropionic acid; EMA, European medicines agency; ESI, Electrospray ionization; FA, Formic acid; HILIC, Hydrophilic interaction chromatography; SHS, Sodium-1-hexanesulphonate, ICH: International conference on harmonization; IPR, Ion pairing reagent; IT, Ion trap; LC, Liquid chromatography; LC/MS, Liquid chromatography coupled to mass spectrometry; LC–UV, Liquid chromatography coupled to ultraviolet detection; MDR-TB, Multidrug resistant tuberculosis; MS, Mass spectrometry; MS^n, Multi-stage mass spectrometry; NMR, Nuclear magnetic resonance; RP, Reversed phase; TOF, Time-of-flight; TUB, Tuberactinomycin; UNK, Unknown; VIO, Viomycin; WHO, World Health Organization

* Corresponding author. Tel.: +32 16323440; fax: +32 16323448.
E-mail address: Erwin.Adams@pharm.kuleuven.be (E. Adams).

0039-9140/$ - see front matter © 2012 Published by Elsevier B.V.
http://dx.doi.org/10.1016/j.talanta.2012.07.090

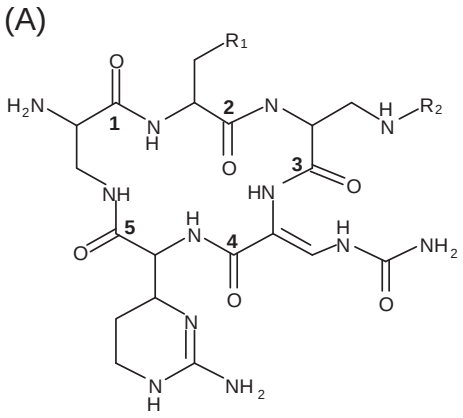

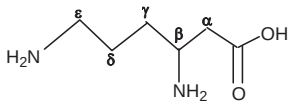

residue6

CMN components	R_1	R_2
IA	OH	β-lysine
IB	H	β-lysine
IIA	OH	H
IIB	H	H

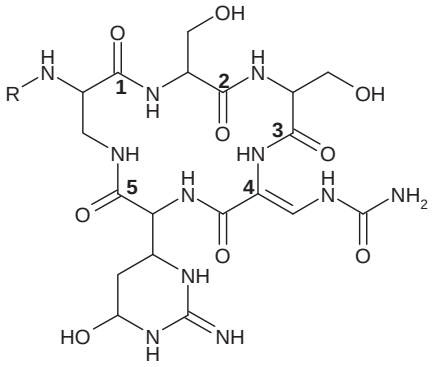

R: β-lysine

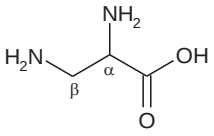

2,3 diaminopropionic acid (DAP)

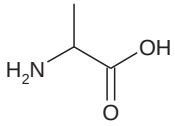

alanine

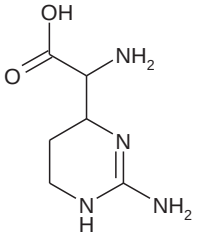

capreomycidine

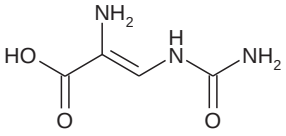

β-ureidodehydroalanine

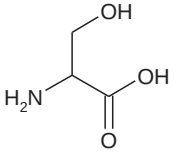

serine

Fig. 1. (A)—Structure of CMN and its components (numbering in the figure corresponds to the residue numbers mentioned in the text); (B)—Structure of viomycin (C)—Structure of some constituent amino acids of the pentapeptide ring of CMN and VIO.

and pasiniazide in urine [10]. Recently, for the first time a RP–LC method for impurity profiling of CMN was described by Mallampati et al. The method could separate the four components of CMN from 11 related substances which were not identified [11]. Also in other literature, no information is available for these or any other impurities present in CMN. The necessity of having this information was clear taking into consideration its importance in the treatment of MDR-TB as it was observed that impurities significantly influence the safety and pharmacokinetic profiles of CMN [9]. A possible explanation for the lack of information regarding the impurities in CMN could be that most of the official methods still recommend thin layer chromatography for its quality control.

On the other hand, drugs must also comply to guidelines of regulatory authorities like ICH (International Conference on Harmonization), which requires that all impurities, above a threshold of 0.1% should be characterized. Although the antibiotics produced by fermentation are not really within the scope of these ICH guidelines,

information regarding the structure of the unknown (UNK) impurities present in them can be useful for ensuring safe and efficacious drug therapy. Recently, the European Medicines Agency (EMA) published guidelines suggesting thresholds for reporting, identification and qualification of related substances in antibiotics produced by fermentation. These guidelines suggest for antibiotics (containing one or more than one active component), produced by fermentation, an identification threshold of 0.15% for their related substances [12].

As several impurities were unknown in the method of Mallampati et al. [11], in this work it was tried to characterize those impurities using ion-trap (IT) MS. To do this, it is interesting to know the fragmentation pattern of the main components which can be used as interpretative templates. Since no data about this were found in literature, the main components were studied first by MS. Next, as many impurities as possible were investigated, even if their content was lower than the thresholds of 0.1% (ICH) and 0.15% (EMA). This was done because the production of antibiotics by fermentation involves biological systems which are complex, less controllable and predictable than chemical synthesis. So, this can result in variable amounts of impurities in different batches of the same drug. As the mobile phase of the Mallampati et al. method, used for separation of impurities in CMN from its main components, had non-volatile constituents, it was not possible to directly send the eluent of the LC–UV to the MS for impurity characterization. Hence an offline approach was applied where the impurity peaks were first collected and salts as well as IPRs (ion-pairing reagents) removed from them before sending them to MS for characterization.

2. Experimental

2.1. Reagents and samples

Acetonitrile (ACN) MS grade and formic acid (FA) 99% ULC/MS grade were purchased from Biosolve LTD (Valkenswaard, the Netherlands). LC gradient grade ACN was purchased from Fischer Scientific (Leicester, United Kingdom). Sodium-1-hexanesulphonate (SHS), phosphoric acid (85% m/m) and potassium dihydrogen phosphate were obtained from Acros (Geel, Belgium). Nitrogen supplied by Air Liquide (Liège, Belgium) was used as sheath and auxiliary gas for MS. Helium gas was purchased from Air Products (Brussels, Belgium). Water was produced in-house by further purifying demineralised water using a Milli-Q Gradient water purification system (Millipore, Bedford, MA, USA). The CMN sample was obtained from WHO (Geneva, Switzerland).

2.2. Liquid chromatographic instrumentation and conditions

2.2.1. Instrumentation and chromatographic conditions for the LC–UV system used for collecting the impurity peaks

An LC–UV system from Dionex (Germering, Germany) was used for separating the peaks using the non-volatile eluent described by Mallampati et al. [11]. The peaks of interest were collected as fractions. A P680 HPLC pump delivered the mobile phase, an automated ASI-100 autosampler injected the samples and an ultraviolet detector (UVD 170U) set at 268 nm recorded the signal. Data acquisition software was Chromeleon (version 6.8, Dionex). As stationary phase, a Hypersil base deactivated C18 column (250 mm × 4.6 mm, 5 μm) was used. It was kept in a water bath maintained at a temperature of 25 °C using an immersion circulator (Julabo EC, Germany). Injection volume was 20 μL. Two mobile phases consisting of ACN-phosphate buffer pH 2.3 with 0.025 M SHS, (A) (5:95, V/V) and (B) (15:85, V/V) were used with the gradient program (Table 1) and delivered at a flow rate of 1.0 ml/min. The mobile phases were degassed by sparging helium. pH measurements were performed on a Metrohm 691 pH meter (Herisau, Switzerland). At the pH of the mobile phase, CMN is protonated and forms ion pairs with the negatively charged SHS which is present in the mobile phase. This mechanism helps in the retention as well as in the separation of CMN from its related substances by the non-polar stationary phase.

Table 1
Gradient program used in the LC–UV method of Mallampati et al. [11].

Time (min)	Mobile phase A (% V/V)	Mobile phase B (% V/V)
0–25	55 to 52	45 to 48
25–40	52	48
40–60	30	70
60–70	55	45

2.2.2. Instrumentation and chromatographic conditions for LC/MS

The impurity peaks that were collected using the previously described LC–UV system were desalted and the analyte molecules separated from SHS prior to their analysis by MS. For this purpose, another LC system was utilized consisting of a Dionex P680 HPLC pump, a manual injector (VICI AG International, Schenkon, Switzerland) equipped with a 500 μL loop and two detectors in series: first a variable wavelength TSP spectra 100 UV–vis detector (San Jose, CA, USA) and second an LCQ MS (Thermo Finnigan, San Jose, CA, USA). Chromeleon version 6.8 (Dionex) was used for recording the signals of the UV detector and Xcalibur 1.3 software (Thermo Finnigan) was used for MS control, data acquisition and processing.

2.2.3. Peak collection and desalting procedure for impurity characterization by LC/MS

To ensure the investigation of a maximum number of impurities in CMN by LC/MS, different CMN samples were screened using the LC–UV method described in 2.2.1 and the sample most rich in impurities was selected. A typical chromatogram is shown in Fig. 2. The sample analyzed by us now showed more impurities than reported by Mallampati et al. for CMN. Peaks above 0.05% (calculated by normalization) were numbered and further investigated. For collection of the impurity peaks, a higher quantity of the sample (50 μL of 2 mg/ml CMN solution) was injected. Elution was followed by monitoring the UV detector signal on the computer. When the UV signal rose, fractions were collected in vials from the outlet of the UV detector and this was stopped when the signal was at the baseline again. Since 100 μg of the sample was injected, an impurity peak of 0.1% would contain approximately 0.1 μg of the analyte of interest. The quantities of impurities in other fractions can be calculated in a similar manner taking into account the percentages based on internal normalization that are indicated in Table 2.

The collected fractions contained the analyte of interest along with non-volatile mobile phase constituents like phosphate buffer and SHS. So, direct coupling of this LC system to MS was not possible. This hurdle can be overcome by a desalting and IPR removal procedure prior to analysis by MS. Desalting of impurity peak fractions was easily achieved, but more difficult was the removal of the IPR. The pH gradient approach described by Pendela et al. for the removal of IPR from streptomycin impurities using a Supelcosil ABZ+ column was taken as starting point [13]. However, using this procedure the m/z ratios of CMNs were not observed in the MS spectra. As CMNs are highly polar in nature, it was decided to replace the column by a more polar one with a lower carbon load (Platinum EPS C18 column, 250 × 4.6 mm, 5 μm), expecting that CMNs would be retained more than the IPR. After trying several eluting solvents, CMNs were successfully

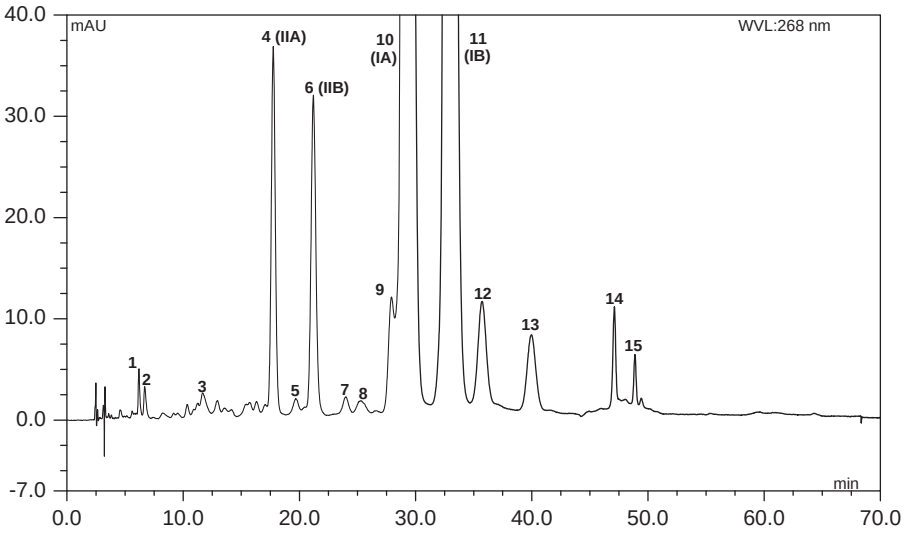

Fig. 2. Typical chromatogram of a capreomycin sulphate sample (2 mg/ml); Peak 4: CMN IIA; Peak 6: CMN IIB; Peak 10: CMN IA; Peak 11: CMN IB; Peaks 1–3, 5, 7–9 and 12–15: unknown impurity peaks.

Table 2
Summary of different *m*/*z* ratios found in CMN impurity peaks, their percentages and the plausible structures assigned to them.

Peak number (percentage of impurities calculated by internal normalization)	Impurity number	*m*/*z*	Proposed name
1 (0.10%)	UNK 1	669	20-*N*-delysine-20-*N*-glutamine CMN IA
2 (0.07%)	UNK 2	653	20-*N*-delysine-20-*N*-glutamine CMN IB
3 (0.17%)	–	–	–
5 (0.11%)	UNK 3	710	13-*N*-glycine CMN IB/ 36-*N*-glycine CMN IB
	UNK 4	740	13-*N*-serine CMN IB/ 36-*N*-serine CMN IB
	UNK 5	770	13-*N*-threonine CMN IA/ 36-*N*-threonine CMN IA
7 (0.12%)	UNK 6	724	13-*N*-alanine CMN IB/ 36-*N*-alanine CMN IB
	UNK 7	754	13-*N*-threonine CMN IB/ 36-*N*-threonine CMN IB
8 (0.13%)	UNK 8	831	derivative of CMN IA
9 (0.71%)	UNK 9	665	28-*N*-methylene CMN IB
12 (1.28%)	UNK 10	669	20-*N*-delysine-36-*N*-lysine CMN IA (isomer of CMN IA)
13 (0.86%)	UNK 11	653	20-*N*-delysine-36-*N*-lysine CMN IB (isomer of CMN IB)
	UNK 12	715	derivative of CMN IB
14 (0.32%)	UNK 13	653	isomer of CMN IB
15 (0.13%)	UNK 14	668	13-*N*-deformamide-13-*N*-acetyl CMN IB/13-*N*-deformamide-36-*N*-acetyl CMN IB

detected using the following conditions. The collected impurity peak fractions were injected using mobile phase A consisting of 0.1% FA:ACN (80:20) at 1.0 mL/min flow rate to elute the salts. At 30.1 min the mobile phase was changed to 100% B (1% FA:ACN (80:20)). The change from 0.1% to 1% FA helped in the elution of CMNs. The initial flow rate of 1.0 mL/min was reduced to 0.2 mL/min when the analyte started eluting (followed by monitoring the signal of the UV detector) and the LC eluent was sent to MS. For all the impurity peaks the same procedure was followed. Each time the column was equilibrated well with mobile phase A before analyzing a new peak fraction.

Different volumes of the impurity peak fractions were injected. In general, 60 μL was injected for larger peaks and 100 μL for smaller peaks. When no *m*/*z* was detected for the smaller peaks, the volume of the fraction was reduced by evaporating some mobile phase using nitrogen so as to increase the concentration of the analyte in the injected fraction.

2.3. Tuning of MS and MS investigation of CMN main components

For tuning of the MS, a solution of CMN having a concentration of 5 μg/mL was infused at a flow rate of 10 μL/min directly into the MS using a built-in syringe pump. It was mixed with the mobile phase (flow rate: 0.2 mL/min) through a T-piece. The LCQ IT MS equipped with electrospray ionization (ESI) was operated in the positive ion mode. The source and the MS parameters were automatically optimized and they are described further. The optimized settings for MS with ESI probe were: sheath and auxiliary gas flow rate 80 and 20 arbitrary units (arb), respectively; spray voltage 4.5 kV, capillary temperature 260 °C, capillary voltage 46.0 V, tube lens offset, 15.0 V, multipole 1 offset, −7.00 V; lens voltage, −16.00 V; multipole 2 offset, −10.00 V, RF amplitude, 580.00 V, peak-to-peak; scan ranges, *m*/*z* 200.00 − 1500.00.

For LC/MS/MS investigation the ions of interest were isolated in the IT with an isolation width of 3 u and activated with 40% collision energy level (CEL). A CEL of 40% was used as it was found to be the optimum amount of energy that generated the highest intensity of the product ion needed for further multi-stage mass spectrometry (MS^n) collision-induced dissociation (CID) experiments.

Besides the data obtained from the LC/MS experiments, the "Fragments & Mechanisms" module in the Mass Frontier software version 2.0 (Thermo Finnigan) was also used for a better understanding of the fragmentation behavior of CMN.

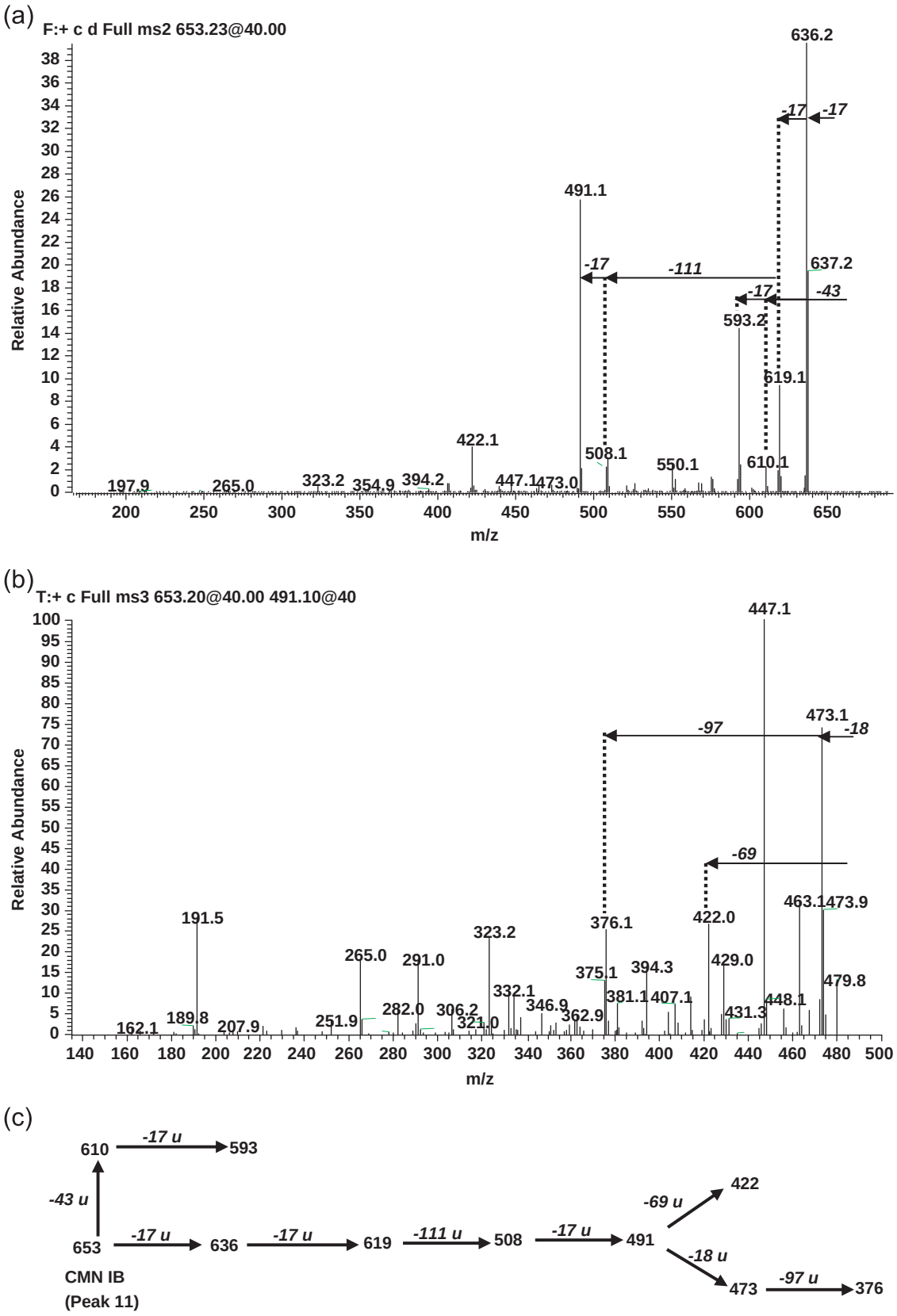

Fig. 3. (a) $[M+H]^+$ CID spectrum acquired for CMN IB (m/z 653), (b) CID MS^n spectrum of $[M+H]^+$ acquired for m/z 653 and (c) Schematic representation of the fragmentation pathways for CMN IB; the result of isolation and collisional activation of the precursor ions in the IT at 40% CEL.

3. Results and discussion

As the impurities of antibiotics (produced by fermentation) are mostly related to the main components, information regarding the fragmentation of the main components can be used for comparison with the fragmentation of impurities which can help in providing beneficial information for the structure elucidation of the UNK impurities.

For CMN, a description of the collision induced spectra of the major component CMN IB along with several other polypeptide antibiotics has been reported by Pittenauer et al. [14]. However, no information was available for the other CMN components. To start, it was decided to study the fragmentation behavior of all the main CMN components, including CMN IB. A problem encountered here was the unavailability of separate reference substances of the main CMN components.

This difficulty was overcome by applying the same procedure of peak collection and desalting for the main components as for the impurities (section 2.2.3), prior to their analysis by MS. Interestingly, in our experiments we were able to obtain more fragments for CMN IB than reported by Pittenauer et al. A description of the fragmentation of the main components of CMN has been given further in the text.

3.1. Fragmentation behavior of the main CMN components: CMN IB (peak 11) ($[M+H]^+$ m/z 653), IA (peak 10) ($[M+H]^+$ m/z 669), II B (peak 6) ($[M+H]^+$ m/z 525) and II A (peak 4) ($[M+H]^+$ m/z 541)

ESI was operated in the positive ion mode and the $[M+H]^+$ precursor ions of CMN IB (*m/z* 653), IIB (*m/z* 525), IA (*m/z* 669) and IIA (*m/z* 541) were isolated with an isolation width of 3 u and collisionally activated at 40% CEL. This was followed by isolation and fragmentation of various product ions that were formed after the loss of neutral fragments from the precursor ion to obtain different order mass spectra.

Based on the information obtained from the mass spectra (Fig. 3), a plausible fragmentation pathway has been suggested for CMN IB which is depicted in Fig. 4 and described further in the text. The fragmentations of the other remaining main components (IIB, IA and IIA) were very similar to that of IB except for a few minor differences which were related to the presence or absence of certain AA residues in their structure. From the suggested scheme it is evident that the fragmentation of CMN molecules mainly involved the cleavage of peptide bonds and losses of several small neutral molecules such as ammonia (involving the various amino groups in the CMN molecule) and water. Peptide bonds are more labile in the positive ion mode of the MS because the amide bond, which is usually stabilized by resonance, gets unstabilized due to protonation of the nitrogen thereby making it more prone to fragmentation [15]. Losses of ammonia and water molecules observed for CMN have also been observed for the fragmentation of the structurally analogous VIO. Also most of the losses described by Pittenauer et al. for CMN were similar to the ones described here [14].

The base peak for protonated CMN IB $[M+H]^+$ was at *m/z* 653. The isolation and collisional activation of the precursor ion led to 2 fragmentation pathways (Fig. 3(c) and Fig. 4). One pathway started with two consecutive losses of 17 u which corresponded to the loss of two of the many amino groups (N-15, N-24, N-28, N-36 or amino at C-7) present in the CMN molecule as ammonia to yield product ions at *m/z* ratios 636 and 619 of which *m/z* 636 had the highest relative abundance. Most likely the loss of N-15 and N-28 amino groups is favored compared to others because of the cleavage of the peptide bond between C-14 and N-15 and the least electron withdrawing effect of the nearest carbonyl (C-21) on the N-28 amino group. Isolation and fragmentation of *m/z* 619 resulted in losses of 111 u (β-lysine without its N-28 amino group) and 17 u (amino as ammonia) forming ions at *m/z* 508 and 491, respectively. The loss of 17 u to form the ion at *m/z* 491 could be either attributed to the amino at N-20 or at N-36. The possibility of N-20 was higher due to less electron withdrawing effect of the nearest C-17 carbonyl group [16]. Next step was the fragmentation of *m/z* 491, which could either undergo two losses: (1) a loss of 18 u (loss of a water molecule involving the oxygen atom at C-1) and 97 u (loss of cyclic guanidine moiety of residue 5) to yield ions at *m/z* 473 and *m/z* 376, respectively, or (2) just a single loss of 69 u to yield a product ion at *m/z* 422. The loss of 69 u could be the result of opening of the pentapeptide core due to the cleavage of the peptide bonds between N-16 and C-17 and N-29 and C-30. Further fragmentation was not successful as these ions were not abundant enough.

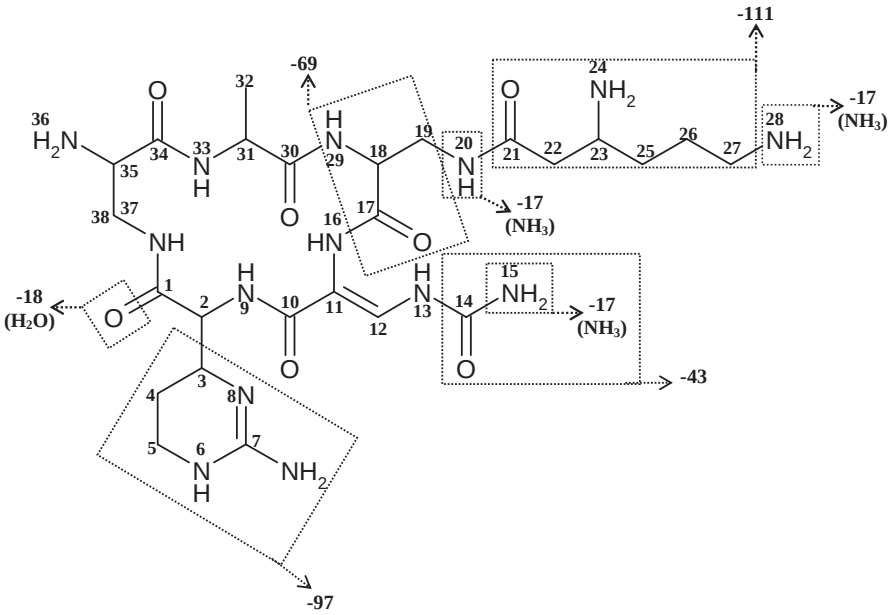

Fig. 4. Plausible fragmentation pathway for CMN IB. The structures were obtained from the Mass Frontier Software.

The other pathway started with the loss of the iminomethanone group (43 u) of residue 4 as a result of the cleavage of the amide bond between N-13 and C-14 to form a product ion at *m/z* 610. This ion further yielded a product ion at *m/z* 593 after losing one of the several amino groups (most likely the N-28 amino group for the same reasons cited above) in the molecule as ammonia (17 u).

The fragmentation of the $[M+H]^+$ precursor ions of CMN IIB and IA (Fig. 5) showed initial losses of 2×17 u ($2\times$ ammonia) involving the loss of the N-15 amino group of residue 4 and the N-28 amino group of residue 6 in IA and the N-15 amino group of residue 4 and the N-20 amino group of residue 3 in CMN IIB. These two losses resulted in product ions at *m/z* 508 and 491 for CMN IIB and at *m/z* 652 and 635 for CMN IA. CMN IIA showed besides the losses of 2×17 u also another pathway (Fig. 5) with sequential losses of 17 u and 18 u (hydroxyl group of residue 2). Next, the product ion from CMN IA at *m/z* 635 lost two fragments of 111 u (residue 6 without its N-28 amino group) and 17 u (loss of N-20 as ammonia) yielding product ions at *m/z* 524 and 507, respectively. These losses were similar to CMN IB, but were not observed during fragmentation of CMN II components. Many significant differences were observed in fragmentation routes of CMN II components from those of CMN I: CMN IA and IB lost three ammonia molecules whereas IIA and IIB lost only two. Loss of an ammonia involving the ε-amino group (N-28) of residue 6 was not observed in case of IIA and IIB as they lack residue 6 (β-lysine). For the same reason there was no loss of 111 u (residue 6 after loss of 17 u from N-28) for CMN II components. Absence of residue 6 also made them more polar leading to earlier elution compared to their CMN I counterparts (retention times: CMN IIA: 18.2 min; CMN IA: 29.1 min; CMN IIB: 21.6 min; CMN IB: 32.9 min) on a reversed phase stationary phase as in the LC–UV method of Mallampati et al. Further fragmentation of *m/z* 491 from CMN IIB resulted in similar losses and product ions compared to that obtained for *m/z* 491 from CMN IB. The product ion at *m/z* 507 from CMN IA, which corresponds to *m/z* 491 of CMN IB, underwent similar losses except that it showed loss of an extra water molecule (18 u) which is logical seen the extra hydroxyl group. Likewise, CMN IIA also showed loss of an extra water molecule (18 u) from its product ion at *m/z* 409 which was formed from *m/z* 506 by the loss of the cyclic guanidine fragment (97 u). The loss of two water molecules in A components compared to the B components was because they contained a serine molecule instead of alanine as residue 2. For the same reason the A components of CMN are 16 u higher in molecular weight than the B components. The presence of serine makes A components more polar than their B counterparts which leads to their earlier elution on a reversed phase stationary phase. A loss of 69 u was also observed in the mass spectrum of CMN IIA which resulted in a product ion (*m/z* 437) but its relative abundance was low.

Similar to the major component CMN IB, the $[M+H]^+$ molecules of CMN IIB, IA and IIA could loose an iminomethanone moiety (43 u) from residue 4 followed by loss of an ammonia molecule (17 u), i.e., the N-28 amino group of residue 6 in IA and the N-20 amino group of residue 1 in IIA and IIB (Fig. 5).

3.2. Investigation of impurities present in a CMN sample

3.2.1. Peak 1 (UNK 1 $[M+H]^+$ *m/z* 669), peak 2 (UNK 2 $[M+H]^+$ *m/z* 653), peak 12 (UNK 10 $[M+H]^+$ *m/z* 669) and peak 13 (UNK 11 $[M+H]^+$ *m/z* 653)

The full mass spectra of UNK 1 and UNK 2 showed the most abundant ions at *m/z* 669 and 653, respectively, which were similar to the *m/z* ratios of CMN IA and IB, respectively. The product ions obtained after isolation and fragmentation of the precursor ions of both UNKs were also similar to those obtained on fragmenting CMN IA and IB. Besides this, they also eluted in pairs and in the same order as IA and IB with the higher *m/z* (UNK 1 at *m/z* 669) eluting before the lower *m/z* (UNK 2 at *m/z* 653). However, their retention time is much shorter, (UNK 1 at 7.2 min and UNK 2 at 7.8 min) compared to IA and IB (Fig. 2). It is suggested that in the two impurities one of the usual AAs of CMN has been replaced by another AA which has the same molecular weight, but is more polar resulting in earlier elution of these impurities on a reversed phase stationary phase. A possibility

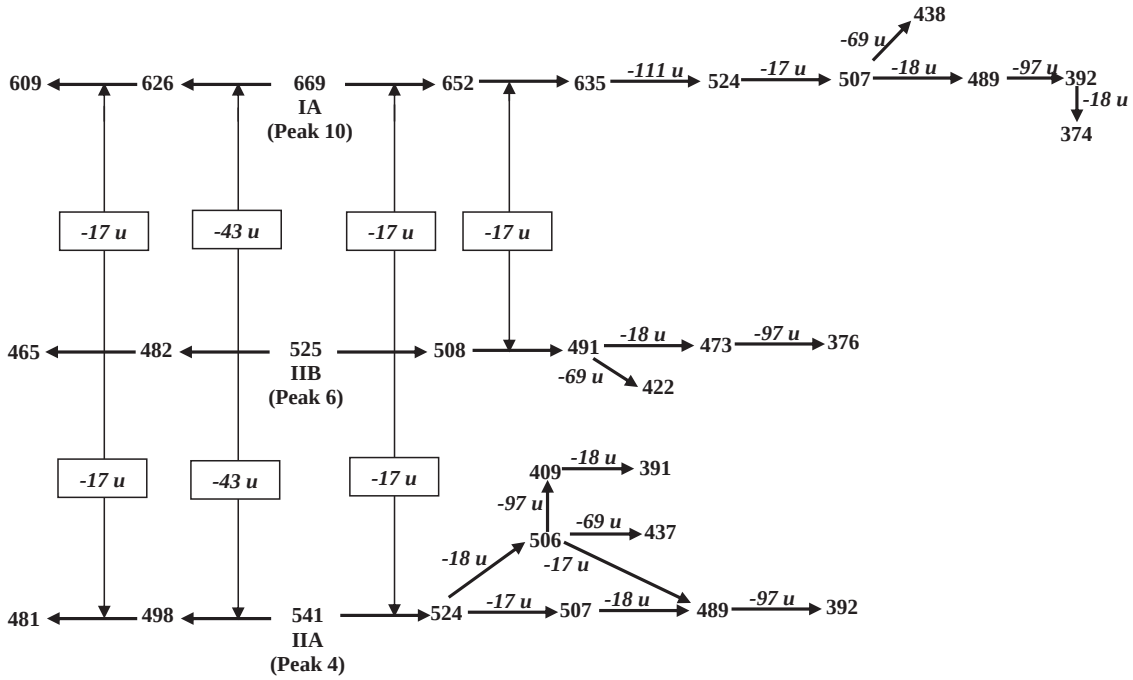

Fig. 5. Schematic representation of the fragmentation of CMN IA, IIA and IIB as a result of isolation and collisional activation of the precursor ions in the IT at 40% CEL.

could be that β-lysine has been substituted by glutamine which has the same molecular weight of 146 u as the former, but is more polar due to a difference in the structure. Glutamine contains an amide and an amino group whereas β-lysine has two amino groups which can form a complex with the IPR at the acidic pH of the mobile phase. Consequently the impurities will interact less with IPR and elute earlier than CMN IA and IB. Thus, the two impurities were suggested to be 20-*N*-delysine-20-*N*-glutamine CMN IA and 20-*N*-delysine-20-*N*-glutamine CMN IB.

Peak 12 shows for $[M+H]^+$ a *m*/*z* of 669 (UNK 10). Peak 13 is the result of coelution of two impurities: UNK 11 and UNK 12. UNK 11 is discussed here while UNK 12 is described later in the text. For UNKs 10 and 11, the situation is similar to UNKs 1 and 2. The most abundant ions in the mass spectra of these two UNKs were at *m*/*z* 669 and 653, respectively. The MS^2 spectra and the elution order of the two UNKs were also similar to that of IA and IB. However, the difference in retention times indicated that the two UNKs were not CMN IA and IB. They can be isomers of IA and IB where β-lysine is linked to the α-amino group of residue 1 (as in the case of other TUBs like viomycin (Fig. 1)) instead of the β-amino group of residue 3 of the cyclic pentapeptide ring. So, plausible structures for UNK 10 and 11 are 20-*N*-delysine-36-*N*-lysine CMN IA and 20-*N*-delysine-36-*N*-lysine CMN IB.

3.2.2. Peak 5 (UNK 3 $[M+H]^+$ m/z 710, UNK 4 $[M+H]^+$ m/z 740, UNK 5 $[M+H]^+$ m/z 770), peak 7 (UNK 6 $[M+H]^+$ m/z 724 and UNK 7 $[M+H]^+$ m/z 754) and peak 13 (UNK 12 $[M+H]^+$ m/z 715)

Peaks 5 and 7 turned out to be a coelution of three and two impurities, respectively, with different *m*/*z* values. The *m*/*z* ratios detected in the first order mass spectrum of peak 5 were 710, 740 and 770 while for peak 7 ions at *m*/*z* 724 and 754 were detected. The mass spectral data of UNKs 3, 4, 6, 7 and 12 could be correlated to the major component CMN IB and they were 57 u, 87 u, 71 u, 101 u and 62 u higher than it, respectively. A schematic representation of the fragmentations of UNKs 3, 4, 6, 7 and 12 is depicted in Fig. 6 (a)). Losses of 17 u, 17 u, 111 u, 17 u, 97 u and 69 u were observed in the MS^2 spectra of all these UNKs. Losses of 43 u and 17 u from the protonated UNKs were also observed. Loss of 18 u was observed in the mass spectra of UNKs 3, 4, 6 and 12. The product ions formed after this loss had low abundance for UNKs 3 and 6. For UNK 7, a loss of 18 u was difficult to ascertain due to low abundance of the resulting ions in the mass spectrum. A major hindrance here was that only limited information was available regarding the fragmentation of the cyclic pentapeptide ring of CMN as neither low-energy CID on an IT, nor high-energy CID on a time-of-flight (TOF) or reflectron TOF instrument can help in cyclic peptide sequencing [14]. In all the UNKs these differences could be due to a single moiety or various groups contributing to the difference. For UNKs 3, 4, 7 and 12, losses corresponding to their difference from CMN IB (i.e., 57 u, 87 u, 101 u and 62 u, respectively) were observed with low abundance in the mass spectral data. So, they could be attributed to single moieties corresponding to the respective molecular weights. For UNK 6 a loss of the extra 71 u could not be observed.

Based on the above observations it is suggested that for UNKs 3, 4, 6 and 7 the difference could be due to the presence of an extra AA: glycine in UNK 3, serine in UNK 4, alanine in UNK 6 and threonine in UNK 7. These AAs are present in the fermentation media used for the growth of micro organisms during the production of antibiotics. For UNK 12, the 62 u difference did not correspond to any AA and the information from the mass spectral data was not sufficient to suggest a possible structure for this moiety.

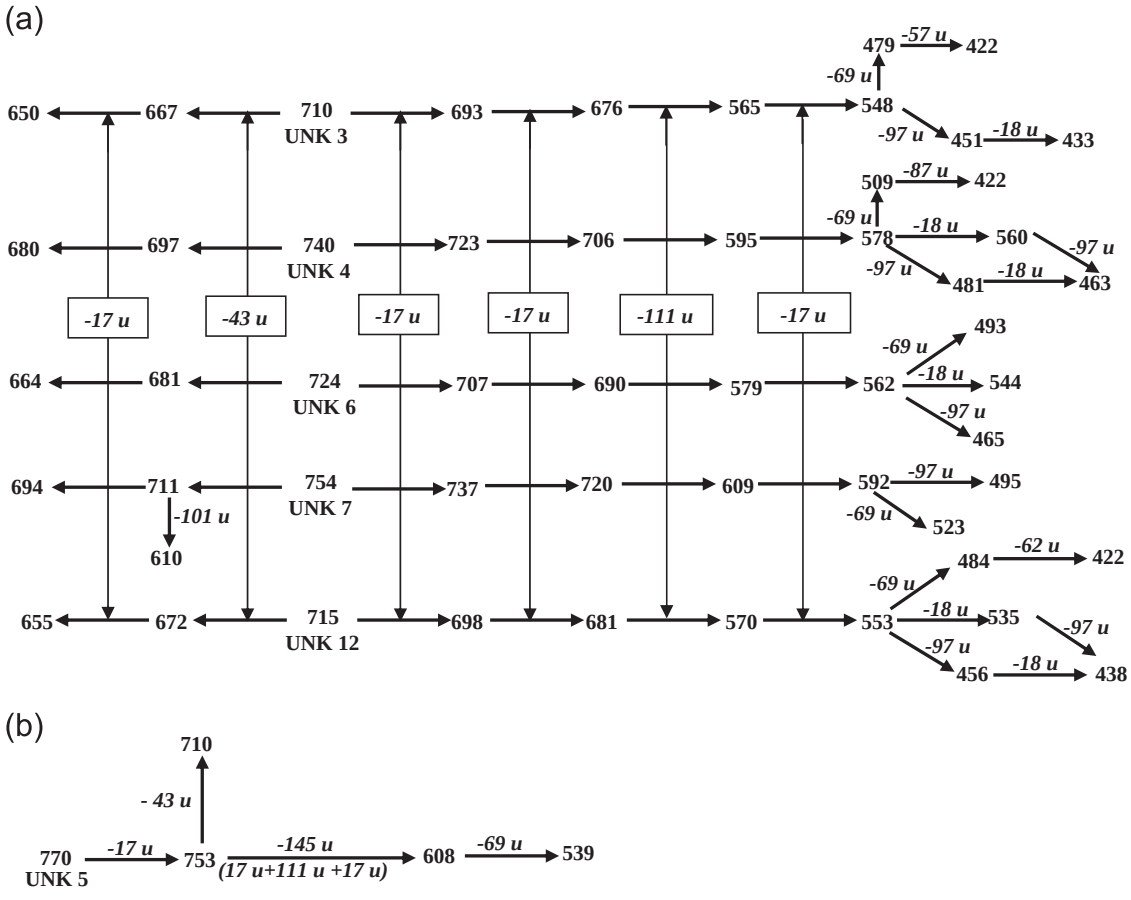

Fig. 6. (a) Schematic representation of the fragmentation of UNKs 3, 4, 6, 7 and 12 and (b) Schematic representation of the fragmentation of UNK 5.

The losses of 17 u, 17 u, 111 u and 97 u in UNKs 3, 4, 6 and 7 ruled out the possibility of amino groups N-15, N-24, N-28 or amino at C-7 being substituted with the above mentioned AAs. So, probably the amino group at N-13 of residue 4 reacts with the various AAs described prior to its carbamoylation to form an ureide structure or another possibility could be the N-36 of residue 1. Thus UNK 3, 4, 6 and 7 can be suggested as 13-*N*-glycine CMN IB or 36-*N*-glycine CMN IB, 13-*N*-serine CMN IB or 36-*N*-serine CMN IB, 13-*N*-alanine CMN IB or 36-*N*-alanine CMN IB and 13-*N*-threonine CMN IB or 36-*N*-threonine CMN IB, respectively.

For UNK 5, only a few losses of 17 u (amino group N-15 or N-28), 145 u and 69 u, were observed in the mass spectrum (Fig. 6 (b)). The loss of 145 u could be due to the combined loss of 17 u (one of the two amino groups, N-15 or N-28, which is not lost in the first step), 111 u (residue 6 without amino group N-28) and 17 u (amino group N-20). Loss of 43 u from its product ion formed after loss of an amino group was also observed. Further losses could not be ascertained due to low abundance of the precursor ions. Based on this data this impurity could either be related to IA or IB. Its *m*/*z* was found to be 101 u higher than CMN IA which corresponds to a threonine molecule as in the case of UNK 7 which was related to CMN IB. Based on the losses observed in the mass spectrum and explanation given above for UNKs 3, 4, 6 and 7, UNK 5 is suggested to be either 13-*N*-threonine CMN IA or 36-*N*-threonine CMN IA. Further confirmation is found in the fact that the CMN IA derivative (UNK 5) is eluted before the analogous CMN IB derivative (UNK 7).

3.2.3. Peak 8 (UNK 8 $[M+H]^+$ *m/z* 831)

The $[M+H]^+$ for UNK 8 was found at *m*/*z* 831, which is 162 u higher than CMN IA. This difference can be explained by observed consecutive losses of 17 u, 18 u and 127 u to yield an ion at *m*/*z* 669, which on further fragmentation gave the product ions characteristic of CMN IA. However, no more information to reveal the structure of this impurity could be obtained from the mass spectra. Further NMR (nuclear magnetic resonance) experiments are suggested for deducing the structure of UNK 8.

3.2.4. Peak 9 (UNK 9 $[M+H]^+$ *m/z* 665)

Compound UNK 9 has a molecular mass 12 u higher than CMN IB. MS^2 investigation of the protonated molecule resulted in a CID spectrum which can be correlated to CMN IB. Fig. 7 shows a schematic view of the fragmentation of this impurity. Comparison of the MS^2 spectrum of UNK 9 and CMN IB revealed that fragmentation of *m*/*z* 631 resulted in product ions at *m*/*z* 508 and *m*/*z* 491 by consecutive losses of 123 u and 17 u whereas the corresponding product ion at *m*/*z* 619 from CMN IB lost 111 u and 17 u to form the same product ions. The CID experiments on *m*/*z* 491 of UNK 9 showed that the losses and product ions formed were similar to those observed for CMN IB. So, except for the loss of 123 u, the losses were similar to CMN IB and indicated that the pentapeptide rings of CMN IB and UNK 9 were composed of the same amino acids. The loss of 123 u in UNK 9 was 12 u more than the loss of 111 u (residue 6 without its N-28 amino group) in case of CMN IB to form the same product ion at *m*/*z* 508. This was indicative of an aberrant residue 6 (β-lysine) in UNK 9. A modification of lysine, with methylene at its N-24 (β-amino group) or N-28 (ε-amino group) can be a possibility. The latter modification with methylene at the ε-amino group, ε-*N*-methylenelysine, which has been described in the literature, is probably present here as well [17]. So, the loss of ammonia (17 u) that was attributed to the N-28 amino group in CMN IB could be due to the N-24 amino group in UNK 9. Also, the loss of 123 u that was analogous to the 111 u (β-lysine without its N-28 amino group) loss observed in CMN IB could be attributed to the aberrant β-lysine (ε-*N*-methylene lysine) without its N-24 amino. So, a plausible structure suggested for UNK 9 is 28-*N*-methylene CMN IB.

3.2.5. Peak 14 (UNK 13 $[M+H]^+$ *m/z* 653)

UNK 13 showed a $[M+H]^+$ at *m*/*z* 653. MS^2 investigation of the protonated molecule resulted in a mass spectrum which had the same ions characteristic to CMN IB fragmentation. This indicated that UNK 13 is probably an isomer of CMN IB which is less polar than IB as it elutes later. NMR experiments are necessary for further confirmation of the structure.

3.2.6. Peak 15 (UNK 14 $[M+H]^+$ *m/z* 668)

The $[M+H]^+$ of UNK 14 at *m*/*z* 668 is 1 u less compared to CMN IA. Isolation and multiple fragmentation of UNK 14 resulted in mass spectral data with losses (17 u, 18 u, 111 u, 17 u, 97 u, 18 u and 69 u) similar to CMN IA (Fig. 8). Besides the above mentioned losses, a loss of 59 u was quite prominent in the mass spectrum of UNK 14 and was not observed for any of the other CMN components. Other differences were also observed, like loss of two ammonia molecules instead of three and absence of a loss of 43 u (iminomethanone of residue 4) as in the fragmentation of CMN IA. These differences indicated that UNK 14 differed from CMN IA with respect to residues 1 and/or 4. It is suggested that residue 4 in this impurity corresponds to α,β-dehydro diaminopropionic acid, the precursor of β-ureidodehydroalanine due to which the loss of 43 u was not observed for UNK 14 [3]. This could also account for the losses of only two ammonia molecules in this impurity compared to the usual three due to absence of N-15 amino group. The loss of 59 u could be attributed to an acetylated amino group with a loss of acetamide during fragmentation. Losses of 17 u, 111 u and 97 u ruled out the possibility of amino

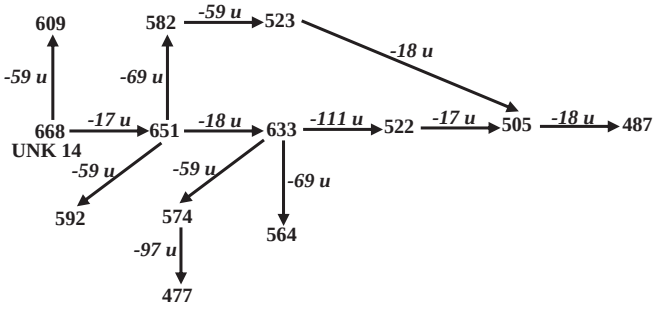

Fig. 8. Schematic representation of the fragmentation pathway for UNK 14.

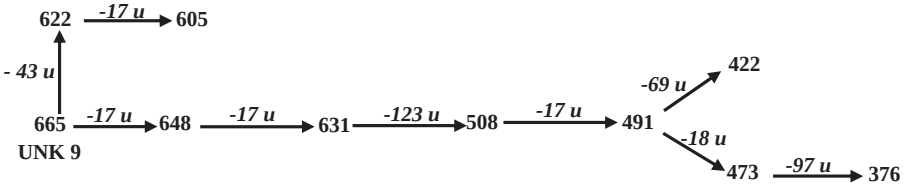

Fig. 7. Schematic representation of the fragmentation pathway of UNK 9.

groups N-24, N-28 and amino at C-7 being acetylated. Combined with the above findings, most likely, the N-13 or the N-36 amino group is acetylated in UNK 14. Acetylation can occur by the enzyme CMN acetyltransferase found in *S. capreolus* [18]. So, plausible structures for UNK 14 can be either 13-*N*-deformamide-36-*N*-acetyl CMN IB or 13-*N*-deformamide-13-*N*-acetyl CMN IB. The more plausible structure is the former one as acetylation of the N-36 amino group of CMN due to the activity of CMN acetyltransferase has been reported by Skinner et al. [18].

3.2.7. Peak 3

When impurity peak 3 was injected into the MS after the removal of buffer salts and IPR, it did not show any abundant *m*/*z*. Several attempts were made to detect the UNK, but they all failed. Probably, the compound of interest could not be separated from the salts and IPR in the second LC system.

4. Conclusion

Though mostly given in combination with other drugs, CMN has gained importance as an essential drug for the treatment of MDR-TB. Its importance has been further stressed by its inclusion in the WHO's list of essential drugs. The development of an LC–UV method for CMN by Mallampati et al. resulted in the separation of its impurities from the main components. However, none of the impurities could be identified. This was the aim of this study. Eleven impurity peaks were separated from the main components in a CMN sample using the LC–UV method. Peaks of interest were collected in fractions and injected in a second LC system to remove salts and IPR before being introduced in the MS. This procedure was successful for all peaks except one (peak 3) for which no *m*/*z* was detected. Some impurity peaks were found to contain more than one impurity. Besides the 4 main components, in total 14 UNKs were found, which were (partly) characterized for the first time. The results obtained are summarized in Table 2. To the best of our knowledge this is the first work aimed at the characterization of the impurities of CMN. The importance of this work lies in the fact that characterization of impurities in drug substances is essential to ascertain and establish the safety and efficacy of drugs as impurities can cause side effects and even be toxic.

References

[1] E.A. Felnagle, M.R. Rondon, A.D. Berti, H.A. Crosby, M.G. Thomas, Appl. Environ. Microbiol. 73 (13) (2007) 4162–4170.
[2] E.B. Herr, M.E. Haney, G.E. Pittenger, C.E. Higgens, Proc. Indiana Acad. Sci. 69 (1960) 134.
[3] M.G. Thomas, Y.A. Chan, S.G. Ozanick, Antimicrob. Agents Chemother. 47 (9) (2003) 2823–2830.
[4] The Merck Index, 14th ed., Merck Research Laboratories, USA, 2006, p. 1753.
[5] D.E. Demong, R.M. Williams, J. Am. Chem. Soc. 125 (2003) 8561–8565.
[6] United States Pharmacopeia, 29th ed., The United States Pharmacopeial Convention, Rockville, 2006, p 363.
[7] British Pharmacopoeia, 3rd ed., British Pharmacopoeia Commission, London, 2003, p. 293.
[8] C. Rossi, G. Fardella, I. Chiapinni, L. Perioli, C. Vescovi, M. Ricci, S. Giovagnoli, S. Scuota, J. Pharm. Biomed. Anal. 36 (2004) 249–255.
[9] S.H. Lee, J. Shin, J.M. Choi, E.Y. Lee, D.H. Kim, J.W. Suh, J.H. Chang, Int. J. Antimicrob. Agents 22 (2003) 81–83.
[10] S.S. Zhang, H.X. Liu, Z.B. Yuan, C.L. Yu, J. Pharm. Biomed. Anal. 17 (1998) 617–622.
[11] S. Mallampati, S. Huang, D. Ashenafi, E. Van Hemelrijck, J. Hoogmartens, E. Adams, J. Chromatogr. A 1216 (2009) 2449–2455.
[12] Guidelines on Setting Specifications for Related Impurities in Antibiotics, European Medicines Agency, 7 Westferry Circus, Canary Wharf, London E14 4HB, United Kingdom, 2010.
[13] M. Pendela, J. Hoogmartens, A. Van Schepdael, E. Adams, J. Sep. Sci. 32 (2009) 3418–3424.
[14] E. Pittenauer, M. Zehl, O. Belgacem, E. Raptakis, R. Mistrik, G. Allmaier, J. Mass Spectrom. 41 (2006) 421–447.
[15] S. Banerjee, S. Mazumdar, Int. J. Anal. Chem. 2012 (2012), Article ID282574.
[16] H. Lioe, R.A.J. O'Hair, Org. Biomol. Chem. 3 (2005) 3618–3628.
[17] E. Floor, A.M. Maples, C.A. Rankin, V.M. Yaganti, S.S. Shank, G.S. Nichols, M. O' Laughlin, N.A. Galeva, T.D. Williams, J. Neurochem. 97 (2006) 504–514.
[18] R.H. Skinner, E. Cundliffe, J. Gen. Microbiol. 120 (1980) 95–104.